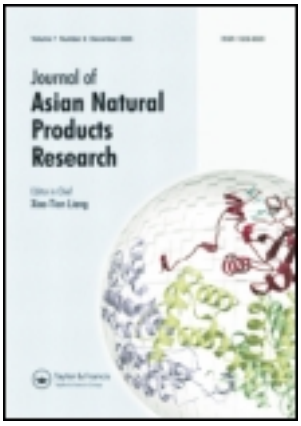

Journal of Asian Natural Products Research

Publication details, including instructions for authors and subscription information:
http://www.tandfonline.com/loi/ganp20

Fully substituted unsaturated lactones from endophytic *Myrothecium* sp.

Hao Xu [a], Nan Jiang [a], Ye Guo [a], Rui-Hua Jiao [a], Jiang-Tao Cui [a], Yong-Chun Song [a] & Ren-Xiang Tan [a]

[a] State Key Laboratory of Pharmaceutical Biotechnology, Institute of Functional Biomolecules, Nanjing University, Nanjing, 210093, China

Available online: 10 Oct 2011

To cite this article: Hao Xu, Nan Jiang, Ye Guo, Rui-Hua Jiao, Jiang-Tao Cui, Yong-Chun Song & Ren-Xiang Tan (2011): Fully substituted unsaturated lactones from endophytic *Myrothecium* sp., Journal of Asian Natural Products Research, 13:11, 1003-1007

To link to this article: http://dx.doi.org/10.1080/10286020.2011.605356

Journal of Asian Natural Products Research
Vol. 13, No. 11, October 2011, 1003–1007

Fully substituted unsaturated lactones from endophytic *Myrothecium* sp.

Hao Xu, Nan Jiang, Ye Guo, Rui-Hua Jiao, Jiang-Tao Cui, Yong-Chun Song and Ren-Xiang Tan*

State Key Laboratory of Pharmaceutical Biotechnology, Institute of Functional Biomolecules, Nanjing University, Nanjing 210093, China

(*Received 9 May 2011; final version received 12 July 2011*)

Two new α,β-unsaturated γ-lactones, myrolactones A (**1**) and B (**2**), were characterized from the culture broth of the *Myrothecium* sp. IFB-E106 isolated from the roots of *Vatica mangachapoi* Blauco. The absolute configuration was determined by the computational electronic circular dichroism approach. Myolactone B showed neuraminidase inhibitory activity with the IC_{50} value of 13.95 μM.

Keywords: *Myrothecium* sp. IFB-E106; α,β-unsaturated γ-lactone; absolute stereochemistry; neuraminidase inhibitor

1. Introduction

Since the discovery of penicillin, the microbial metabolites have been explored for pharmaceutical agents such as antibiotics, immunomodulators, enzyme inhibitors, and anticancer drugs. However, the hitrate is descending if the endeavor is limited to the well-investigated environmental microorganisms. In this dilemma, who is the more profitable producer, endophytes, which are microbes living inside the healthy host plants, are being recognized as a rich source of functional biomolecules [1,2]. Among the endophyte community, the *Myrothecium* sp. behaves unique in its production of arrays of bioactive secondary metabolites including macrocyclic trichothecenes, such as verrucarins, roridins, satratoxins, miotoxins, roritoxins, mytoxins, and myrotoxins [3,4]. As an immediate follow-up to our characterization of new bioactive metabolites from endophytic *Cochliobolus* sp. [5] and mantis-associated fungus [6], we investigated the new bioactive metabolites produced by *Myrothecium* sp. IFB-E106 residing originally inside the root of *Vatica mangachapoi* Blauco, with an intention to characterize microbial modulator(s) of neuraminidase, a key enzyme involved in the respiratory infection due to influenza virus [7]. As a result, two new compounds named myrolactones A (**1**) and B (**2**) were afforded, with the latter ascertained to be a neuraminidase inhibitor (Figure 1).

2. Results and discussion

Myrolactone A (**1**, white powder) was disclosed to have a molecular formula of $C_8H_{12}O_4$ by its high-resolution electrospray mass spectrum (HR-ESI-MS). The ^{1}H NMR spectrum of **1** exhibited a few singlets indicating presumably the presence of two methyl (δ 1.67 and 1.97), a methoxyl (δ 3.24), an oxomethylene (2H, δ 4.50), and a hydroxyl (1H, δ 2.13, broadened) groups. The assumption was

*Corresponding author. Email: rxtan@nju.edu.cn

ISSN 1028-6020 print/ISSN 1477-2213 online

http://dx.doi.org/10.1080/10286020.2011.605356
http://www.tandfonline.com

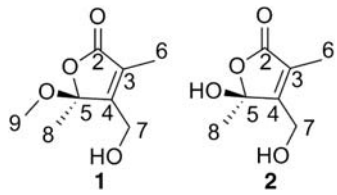

Figure 1. Structures of myrolactones A (**1**) and B (**2**).

reinforced by its ^{13}C NMR spectrum that gave, as edited by the distortionless enhancement by polarization transfer pulse sequence, a total of eight carbon resonance lines consisting of two methyl (δ 8.7 and 22.7), one methoxyl (δ 50.9), one oxomethylene (δ 56.8), one carbonyl group (δ 171.3), two olefinic (δ 127.9 and 156.5), and one quaternary (δ 107.7) carbons. All ^{1}H and ^{13}C NMR spectral data of **1** were assigned through a combination of HMQC and HMBC experiments (Table 1 and Figure 2). In particular, the structure of **1** was accommodated collectively by the three degrees of unsaturation, the striking difference in the chemical shifts of C-3 (δ 127.9) and C-4 (δ 156.5), along with the HMBC correlations of the carbonyl (C-2, δ 171.3) with H-6 (δ 1.97), of C-3 with H-7 (δ 4.50), of C-4 with H-6 and H-8 (δ 1.67), and of C-5 (δ 107.7) with H-7 and the methoxy proton singlet at δ 3.24 (Figure 2). To elucidate the absolute configuration of the single chiral center (C-5) in the molecule, we acquired the electronic circular dichroism (ECD) spectrum of **1**, which matched well the *S*-configuration counterpart computed as reported (Figure 3) [6,8].

Myrolactone B (**2**, colorless oil) was analyzed by the HR-ESI-MS to have a molecular formula of $C_7H_{10}O_4$, a methylene less than that of **1**. The ^{1}H and ^{13}C NMR spectral data of **2** were closely similar to those of **1** (Table 1). However, the methoxy singlet at δ 3.24 in the ^{1}H NMR spectrum of **1** was missing in that of **2**, indicating that myrolactone B was most probably a 5-*O*-demethyl derivative of myrolactone A. This was substantiated by its HMBC spectrum (Figure 2). The 5*S*-configuration of **2** was also disclosed by comparing its experimental and computational ECD spectra (Figure 4).

The *in vitro* neuraminidase inhibitory test of these two compounds showed that myrolactone B (**2**) was active against the enzyme with an IC_{50} value of 13.95 μM, using as a positive control oseltamivir the IC_{50} of which was 0.14 μM in the same assay. It was surprising that the 5-hydroxy group was so 'essential' for the inhibition of such a key biomolecule that governs the respiratory infection by the influenza virus [7].

3. Experimental

3.1 General experimental procedures

Optical rotations were determined in $CHCl_3$ on a WXG-4 disk polarimeter. UV and IR spectra were recorded on a Hitachi U-3000 spectrophotometer and a Nexus 870 FT-IR

Table 1. ^{1}H and ^{13}C NMR spectral data of **1** ($CDCl_3$) and **2** (methanol-d_4) with *J* in Hz.

	1		**2**	
Position	δ_H	δ_C	δ_H	δ_C
2		171.3		174.2
3		127.9		126.6
4		156.5		161.4
5		107.7		107.3
6	1.97 (s)	8.7	1.92 (s)	8.7
7	4.50 (s)	56.8	4.47 (s)	57.0
7-OH	2.13 (br s)			
8	1.67 (s)	22.7	1.65 (s)	24.8
9	3.24 (s)	50.9		

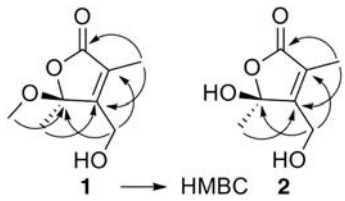

Figure 2. Key HMBC correlations of myrolactones A (**1**) and B (**2**).

spectrometer, respectively. Circular dichroism (CD) spectra were recorded on a Jasco J-810 spectropolarimeter. NMR spectra were recorded on Bruker DPX-300 and DRX-500 NMR spectrometers. HR-ESI-MS were recorded on Agilent 6210 TOF LC/MS. Silica gel (SiO_2, 200–300 mesh) for column chromatography and silica GF254 (10–20 mm) for TLC were obtained from Qingdao Marine Chemical Factory (Qingdao, China). Sephadex LH-20 was obtained from Pharmacia Biotech (Uppsala, Sweden). HPLC was performed with a Hitachi L-7110 pump, and UV detector L-7400 was equipped with an Apollo C18 column (5 μm, 250 × 4.6 mm; Alltech Associates, Inc., Chicago, IL, USA).

3.2 *Fungus material*

The *Myrothecium* strain IFB-E106, maintained on potato–dextrose agar (PDA), was isolated from the roots of *V. mangachapoi* Blauco. After growing on the PDA medium at 28°C for 4 days, plugs of agar supporting mycelial growth were cut and transferred

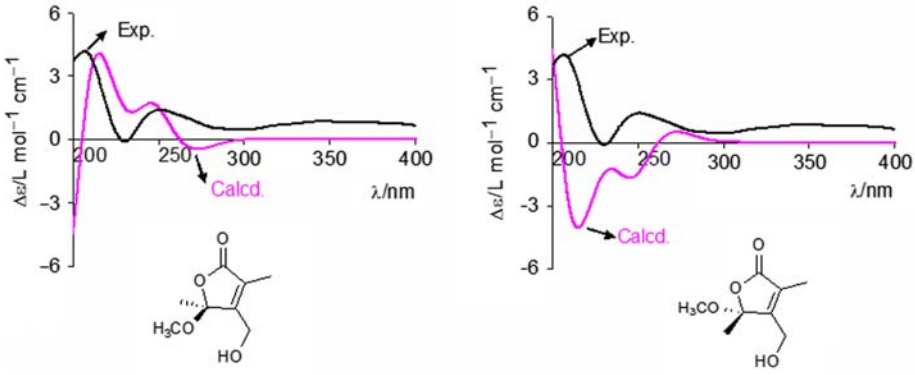

Figure 3. Comparison of the experimental CD spectrum of **1** with those calculated for its optional enantiomers (5*S*)- and (5*R*)-isomers.

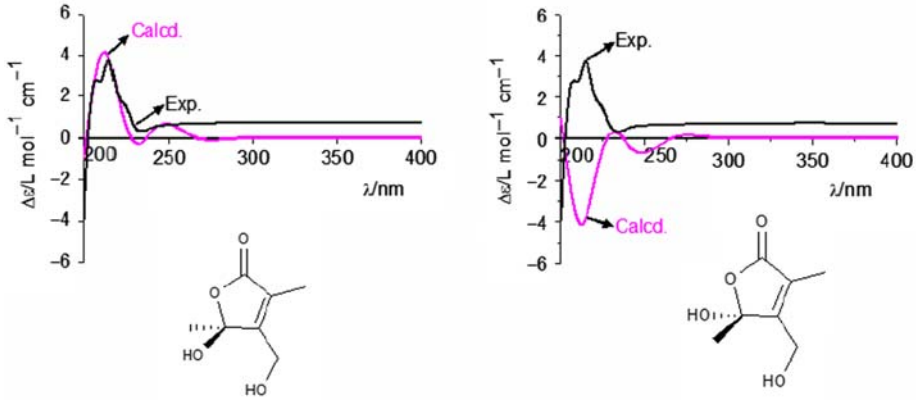

Figure 4. Comparison of the experimental CD spectrum of **2** with those calculated for its optional enantiomers (5S)- and (5R)-isomers.

aseptically into 1000 ml Erlenmeyer flasks preloaded with 300 ml of Czapek liquid medium. The flasks were then incubated at 28 ± 1°C on a rotary shaker at 150 rpm for 14 days.

3.3 Extraction and isolation

The cultures (40 L) were filtered through cheesecloth. The filtrate was extracted five times by shaking with an equal volume of ethyl acetate. Removal of the solvent *in vacuo* gave a residue (10.3 g) that was soaked in MeOH (500 ml) around 60°C. The afforded solution was cooled down gradually to −20°C, which was followed by standing for another 24 h to get rid off lipids and salts that could precipitate. Evaporation of methanol under reduced pressure yielded a residue (6.1 g) that was chromatographed over a silica gel column eluting successively with $CHCl_3$/MeOH (100:0, 100:1, 100:2, 100:4, 100:8, 100:16, and 0:100, v:v) to give seven fractions (Frs 1–7). Fr. 2 (0.8 g) was subjected to gel filtration over Sephadex LH-20 with MeOH to yield two subfractions (Frs 2.1–2.2). Fr. 2.1 (0.4 g) was purified further by HPLC [Hypersil BDS C18 5 μm; MeOH–H_2O (v:v = 60:40); 2.0 ml/min; λ = 254 nm] to afford **1** (14.8 mg, t_R: 18.2 min). Fr. 4 (1.5 g) was also subjected to gel filtration over Sephadex LH-20 with MeOH to yield four subfractions (Frs 4.1–4.4). From Fr. 4.3 (0.4 g), compound **2** (7.2 mg, t_R: 12.4 min) was obtained after purification with HPLC [Hypersil BDS C18 5 μm; MeOH–H_2O (v:v = 35:65); 2.0 ml/min; λ = 254 nm].

3.3.1 Myrolactone A

A white powder ($CDCl_3$). $[\alpha]_D^{20}$ + 109.7 (c = 0.012, MeOH). UV (MeOH) λ_{max} (log ε): 214 (3.42) nm. IR (KBr) ν_{max} 3446, 2995, 2941, 1744, 1458, 1377, 1298, 1186, 1028, 920, 899, 763 cm^{-1}. ^1H and ^{13}C NMR spectral data, see Table 1. HR-ESI-MS *m/z*: 195.0642 $[M + Na]^+$ (calcd for $C_8H_{12}O_4Na$, 195.0633).

3.3.2 Myrolactone B

Colorless oil (MeOH). $[\alpha]_D^{20}$ + 115.2 (c = 0.015, MeOH). UV (MeOH) λ_{max} (log ε): 213 (2.85) nm. IR (KBr) ν_{max} 3346, 2992, 2929, 1743, 1437, 1383, 1266, 1199, 1044, 950, 904, 767 cm^{-1}. ^1H and ^{13}C NMR spectral data, see Table 1. HR-ESI-MS *m/z*: 181.0464 $[M + Na]^+$ (calcd for $C_7H_{10}O_4Na$, 181.0477).

3.4 Computational details

For these systems, the full geometry optimization was carried out with density functional theory (DFT) at B3LYP/6–31+G(d,p) level. The solvent effects on the electronic structures of the studied systems were evaluated by quantum chemistry method through polarizable continuum model (PCM) model (dielectric constant ε = 32.63 for CH_3OH). Then, the corresponding excited-state calculations were performed at the ground-state optimized geometries. Time-dependent DFT in combination with PCM model with the same basis set was carried out to calculate the spin-allowed excitation energy and rotatory strength of the lowest 50 excited states. The UV and ECD spectra were generated using the program SpecDis [9] by applying a Gaussian band shape with 0.30 eV width, from oscillator strengths and dipole velocity rotational strengths, respectively. The final ECD spectra were shifted by 10 nm to high wavelength according to UV correction. The optical rotations at the sodium D line were obtained by dipole electric field polarizability calculations at B3LYP/6–31+G(d,p) level using PCM for CH_3OH. All the calculations were performed with the Gaussian 03 program [10].

Acknowledgements

The work was co-supported financially by grants from NSFC (30821006 and 90813036) and MOST (2009ZX09501-013).

References

[1] G. Strobel and B. Daisy, *Microbiol. Mol. Biol. Rev.* **67**, 491 (2003).

[2] H.W. Zhang, Y.C. Song, and R.X. Tan, *Nat. Prod. Rep.* **23**, 753 (2006).

[3] L. Shen, R.H. Jiao, Y.H. Ye, X.T. Wang, C. Xu, Y.C. Song, H.L. Zhu, and R.X. Tan, *Chem. Eur. J.* **12**, 5596 (2006).

[4] L. Shen, J.S. Wang, H.J. Shen, Y.C. Song, and R.X. Tan, *Planta Med.* **76**, 1004 (2010).

[5] Q.Z. Wang, H.M. Ge, J. Zhang, J.H. Wu, Y.C. Song, Y.F. Zhang, and R.X. Tan, *J. Asian Nat. Prod. Res.* **12**, 485 (2010).

[6] Y.L. Zhang, J. Zhang, N. Jiang, Y.H. Lu, L. Wang, S.H. Xu, W. Wang, G.F. Zhang, Q. Xu, H.M. Ge, J. Ma, Y.C. Song, and R.X. Tan, *J. Am. Chem. Soc.* **133**, 5931 (2011), and related references therein.

[7] R.J. Jackson, K.L. Cooper, P. Tappenden, A. Rees, E.L. Simpson, R.C. Read, and K.G. Nicholson, *J. Infect.* **62**, 14 (2011).

[8] N. Jiang, R.X. Tan, and J. Ma, *J. Phys. Chem.* **115B**, 2801 (2011).

[9] T. Bruhn, Y. Hemberger, A. Schaumlöffel, and G. Bringmann, *SpecDis version 1.50* (University of Wuerzburg, Germany, 2010).

[10] M.J. Frisch, G.W. Trucks, H.B. Schlegel, G.E. Scuseria, M.A. Robb, J.R. Cheeseman, J.A. Montgomery Jr, T. Vreven, K.N. Kudin, J.C. Burant, J.M. Millam, S.S. Iyengar, J. Tomasi, V. Barone, B. Mennucci, M. Cossi, G. Scalmani, N. Rega, G.A. Petersson, H. Nakatsuji, M. Hada, M. Ehara, K. Toyota, R. Fukuda, J. Hasegawa, M. Ishida, T. Nakajima, Y. Honda, O. Kitao, H. Nakai, M. Klene, X. Li, J.E. Knox, H.P. Hratchian, J.B. Cross, V. Bakken, C. Adamo, J. Jaramillo, R. Gomperts, R.E. Stratmann, O. Yazyev, A.J. Austin, R. Cammi, C. Pomelli, J.W. Ochterski, P.Y. Ayala, K. Morokuma, G.A. Voth, P. Salvador, J.J. Dannenberg, V.G. Zakrzewski, S. Dapprich, A.D. Daniels, M.C. Strain, O. Farkas, D.K. Malick, A.D. Rabuck, K. Raghavachari, J.B. Foresman, J.V. Ortiz, Q. Cui, A.G. Baboul, S. Clifford, J. Cioslowski, B.B. Stefanov, G. Liu, A. Liashenko, P. Piskorz, I. Komaromi, R.L. Martin, D.J. Fox, T. Keith, M.A. Al-Laham, C.Y. Peng, A. Nanayakkara, M. Challacombe, P.M.W. Gill, B. Johnson, W. Chen, M.W. Wong, C. Gonzalez, and J.A. Pople, *Gaussian 03; Revision D. 01* (Gaussian, Inc., Wallingford, CT, 2004).